Modeling the 2017 September 10 LDGRF

James M. Ryan (UNH), Georgia A. de Nolfo (GSFC), Dale E. Gary (NJIT)

University of New Hampshire

Abstract

The series of large flares from 2017 September 4 to 10 were significant microwave events with revealing multi-wavelength images of the flare environment. The event on September 10 was a large long-duration, gamma-ray flare (LDGRF). The event also produced a Ground Level Enhancement (GLE). Using the microwave imaging data from the Expanded Owens Valley Solar Array (EOVSA) we interpret and model the behavior of the energetic-flare protons of September 10 as measured with the Large Area Telescope (LAT) on the Fermi mission. We do this in the context of stochastic acceleration in a large coronal bipolar structure to produce the high-energy long-duration γ-ray emission. Our preliminary analysis suggests that the acceleration of the GeV protons takes place in a large structure about 1.4 $R_\odot$ in length. The requirements for the magnetic field and turbulence in this structure are presented.

Objectives

Long Duration Gamma-Ray Flares (LDGRF) exhibit a delayed onset and emit very high energy γ rays. It has been postulated from the first observations that the same particles that produce ground level enhancements (GLE) also produce the γ radiation from the Sun. However, the phenomenon is frequent, robust and repeatable. Modeling the necessary particle transport from great distances once accelerated in an IP shock is strained. Magnetic connections to the shock front are transient and the diffusion through the downstream region to the solar surface from distances as long as a fraction of an AU would seem to be unreliable, given the magnetic re-structuring taking place behind the CME. Furthermore, one must produce a profile that is remarkably diffusive in nature, no bump, no wiggle—a pure exponential for many hours.

Alternatively, we can investigate a diffusion solution to the particle transport and acceleration as it can take place in large coronal loops, distinct from the receding CME and shock. Modeling by Ryan and Lee (1991) shows that the trapping volumes must be large and filled with MHD turbulence to accelerate the ions via second-order Fermi acceleration and transport them diffusively to the solar photosphere where they radiate for long periods. Lacking, though, is a visualization of such an active loop that could be the home and the accelerating agent for the protons. The unique microwave observations of the 2017 September flares reveals loops of the appropriate size and location, allowing us to model the acceleration and transport.

The 2017 September events were bona fide LDGRFs with accompanying energetic ions detected in space. The loops of this event are luminous in microwaves through the emission by energetic electrons and positrons. We can, thus, set constraints on the necessary embedded (and largely invisible) turbulence.

We search for a self-consistent, data-supported diffusion model of the LDGRF process without invoking a distant receding shock.

Observations and Modeling

The 2017 September 10 event was an unusually powerful LDGRF, emitting >100 MeV γ rays for several hours. Perhaps due to connectivity, it was a somewhat less impressive GLE and solar energetic particle (SEP) event at Earth (Bruno et al. 2018). Being on the west limb with coronal loop structures oriented with a significant north-south orientation, the event was seen in profile by EOVSA (Gary et al. 2018), allowing an examination of the dimensions of the affected volumes in the corona. Shown below left is the entire-event γ-ray photometry curve >100 MeV. Below right is a snapshot of the 3.4-GHz microwave emission early in the event. It shows, in the red curves, the legs of a loop we believe contains the energetic particles necessary for the LDGRF.

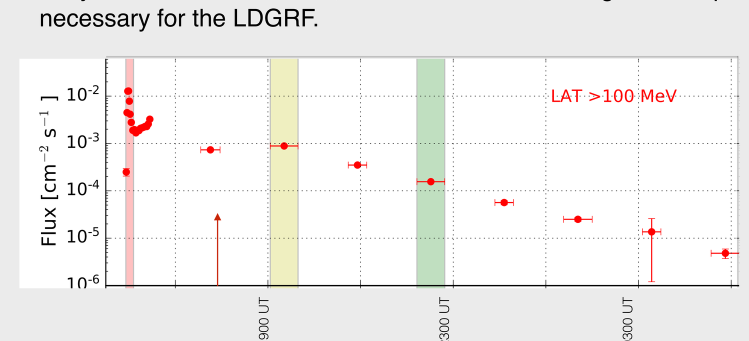

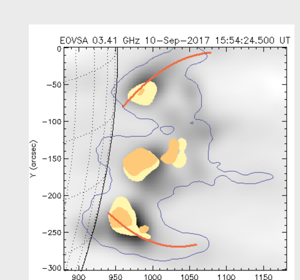

We focus on the period after 1900 UT on September 10 that exhibits a smooth photometric exponential decay (±20%) with a time constant of ~6500 s, for >10 hours, while the spectral index softens from 3.7 to 6 (Omodei et al. 2018). This period was also chosen because it is well after any disturbance produced by reconnections in and around the smaller loop and well after any CME. There is other activity leading up to the decay, including an impulsive phase and an intermediate recovery and fall (hidden by Earth occultation) that gives way to the gradual feature. The onset of the long duration phase appears to have started some time earlier than 1900 UT. That corresponding image at 1800 UT, prior to the smooth decay phase, is shown below. The figure is the AIA (171 Å) superposed on that of the EOVSA 3.9-GHz image near the peak of the gradual phase. It is important to note that acceleration after 1900 UT is still necessary. No form of passive trapping can support a population for 10 hours without enormous (many AU) scattering mean free paths.

The 3.4-GHz image at 1600 UT above defines the relevant structures and their dimensions. There is an inner reconnection structure that can be seen below at 1800 UT. The red curves in the 3.4-GHz image above are indicated as likely legs of a single larger loop. In particular, the separation of the most northern and southern lobes of this larger loop is of order 175″ or 0.2 $R_\odot$ in the plane normal to the observer. We take these to be the feet of a larger loop-like structure. We estimate that the loop reaches a height of 0.4 $R_\odot$ with a circular length of 1.4 $R_\odot$. At 1800 UT, and thereafter, the μ-wave and HXR activity is confined to the smaller central loop and is thermal in nature (20 MK), as is the x-ray emission (Omodei et al. 2018).

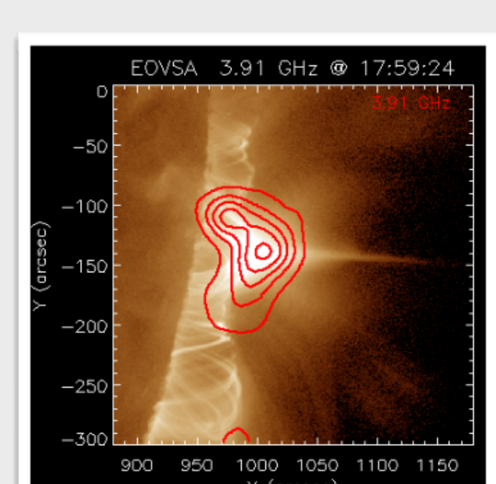

After 1800 UT no measurable non-thermal emission is detectable in the field of view of the observing instruments, other than the 100-MeV γ-ray emission. This behavior is similar to earlier non-imaging observations. Unfortunately, little information comes from the γ-ray image produced by Fermi/LAT at the time of the green bar in the Fermi/LAT photometric plot (Omodei et al. 2018). The error circle of the 100 MeV emission from LAT is large enough late in the event to capture the large loops, but this may only reflect the poorer statistics late, rather than true extended emission.

Modeling

The model, in its simplest, form is a 1-d leaky box, if one only considers the long-term decay, neglecting the early time dependent aspect of the problem, i.e., the initial acceleration and transport of the particles to the footpoints, where they radiate (Ryan and Lee 1991). The initial acceleration and transport to the footpoints is present before 1900 UT, where the emission is intensifying. The diffusion, assuming $\lambda \ll \ell$, where λ is the particle mean free path and ℓ is the length of the trapping volume, governs the physical transport of the particles. It also is responsible for the acceleration of the protons via the second-order Fermi process, the time scale of the acceleration is inversely proportional to the spatial diffusion time. If we further assume that the spectral shape is stationary (which it is not, see below) then this decay in a linear box of length l is governed only by the measured spatial diffusion time constant $\tau_d = \ell^2/\pi^2\kappa$, where κ is the inferred or measured spatial diffusion coefficient, assumed to be momentum or energy independent. The quantity κ, however, does not fully capture the observed decay of the particle distribution. The value of κ should be considered an upper limit, because acceleration continues during the transport and the precipitation process. That said, we take the acceleration rate with respect to the loss rate to be stabilized and that the spectral shape of the ions above the γ-ray production threshold (~300 MeV) is steady. The softening of the spectrum with time measured by Fermi/LAT, however, belies this assumption to some degree, but probably not too much, given that the spectrum is still well represented by a power law. In summary, if one knows both ℓ and τ_d, one can deduce κ, the diffusion coefficient. In our case, neglecting acceleration, the gradual phase time constant is ≲6500 s from which we compute κ. Quasi-linear theory can be used to estimate some plasma properties within the trap, such as $\delta B/B$, and from that the spectrum-integrated wave-energy density (e.g., Lee, 1982).

A 6500-s precipitation of particles to the footpoint in a loop of length 1.4 $R_\odot$ requires a diffusion coefficient of 1.4×10^{17} cm^2-s^{-1}, corresponding to λ~200 km, consistent with the diffusion approximation.

To see how much wave intensity we need, we normalize the wave power spectrum to the intensity at the resonant wave number in a 1-G field. From there we extend the $k^{-5/3}$ Kolmogorov form to a k value representative of the loop cross section diameter that we take to be $\ell/10$, where it is flat to the origin. This in turn implies a wave field energy of 0.7 ergs-cm^{-3}, which exceeds the ambient magnetic field energy at 1 G (0.04 ergs-cm^{-3}), what we might expect at an altitude of 0.4 $R_\odot$. However, no such problem exists farther down the legs of the loop, where B is much greater. For example, when B~10 G, only 18% of the ambient B energy need be in the form of waves. The situation improves rapidly with increasing B in a dipolar field.

Discussion

Are we accelerating particles? An acceleration time scale τ_a ($=9\kappa/V_A^2$) (Schlickeiser 1986) can be computed. For the acceleration time scale to equal the diffusion time scale, one needs an Alfvén speed >140 km-s^{-1}, a modest requirement. Greater speeds shorten τ_a.

This simple analysis reveals several things:

i. With unprecedented μ-wave imaging, we can put realistic numbers on coronal traps that can produce protons of sufficient energy to power an LDGRF.

ii. Accompanying images and data from SDO, RHESSI and LAT allow us to quantitatively examine the energetic particle environment.

iii. We see that diffusion in a static loop can successfully both impede the transport of particles and accelerate them to the requisite energy.

However, this new information highlights shortcomings of the model.

i. Grechnev et al. (2018) concluded that a shock passage seeds the large loop, in which the diffusion process occurs. This event is similar, in that, the reconnection site associated with the central HXR, AIA and μ-wave image gives rise to a breakout process (Karpen et al. 2018), producing a shock that likely accelerates particles to modest energy at low altitudes. However, after 3 hours, the region behind the blob will likely re-configure into a more dipole like structure. This leaves behind a large loop with seed particles, with those particles being unrelated to those in the impulsive phase, reminiscent of Hudson's lasso picture (Hudson 2018).

ii. The model is too simple as is. For large loops we must incorporate the inhomogeneity of magnetic field.

iii. In regions where B is too small to support the necessary wave field, the containment of the wave energy must be included, perhaps similar to that discussed by Hollweg (1984) where waves in loops are reflected off gradients and discontinuities in the "index of refraction."

iv. Investigate self-generated waves produced by the low-energy protons that resonate with higher energy protons, producing a non-Kolmogorov spectrum, similar to that computed by Lee (1982).

v. One must include a momentum-dependent diffusion coefficient that will produce a varying power law spectral index.

Conclusions

Conceptually and qualitatively, a coronal trap, with spatial and momentum diffusion governing the precipitation of high-energy particles, can re-produce LDGRF behavior witnessed since 1982 (Chupp et al. 1983). The diffusive behavior produces a "perfect" exponential decay, difficult to achieve by other processes. Realistic numbers obtained from new measurements of an actual environment clears the way for future modeling efforts.

References

1. Bruno, A. et al. 2019, *Space Weather*, **17**, 418.
2. Chupp, E.L. and J.M. Ryan 2009, Res. in Astron. and Astrophys., **9**.
3. Chupp, E.L. et al. 1987, Astrophys. J., **318**.
4. Gary et al., 2018, Astrophys. J., 863, **83**.
5. Grechnev et al. 2018, Solar Phys., **293**, 133.
6. Hollweg, J. 1984, Astrophys. J., **91**, 269.
7. Hudson, H. 2018, Proceedings of IAU Symp. No. 335, **49**.
8. Karpen, J. et al., 2019, Bull. Am. Astron. Soc., **51**.
9. Lee, M.A. 1982, J. Geophys. Res., **87**.
10. Omodei et al. 2018, Astrophys. J. Lett., **865**, L7.
11. Ryan, J.M. and M.A. Lee, 1991, Astrophys. J., **368**.
12. Schlickeiser, R. 1986, Stochastic Particle Acceleration in Cosmic Objects, in Cosmic Radiation in Contemporary Astrophysics, Reidel.

We thank Dr. M.A. Lee for helpful discussions.

This work was supported by NSF grant 1838512 and NASA grant NNX16AL66G (UNH and GSFC). This research is also supported by NSF grant AST-1615807 and NASA grants 80NSSC18K1128 and 80NSSC19K0068 to New Jersey Institute of Technology.